

# WAVE BREAKING OVER LOCAL TOPOGRAPHY DURING THE MAP IOP 15 MISTRAL EVENT: OBSERVATIONS AND HIGH-RESOLUTION NUMERICAL SIMULATIONS

Vincent Guénard<sup>1</sup>, Gilles Tedeschi<sup>1</sup>, Philippe Drobinski<sup>2</sup>, Jean Luc Caccia<sup>1</sup>

<sup>1</sup> LSEET-LEPI, CNRS, Université du Sud Toulon-Var, Avenue de l'université, BP 20132, 83957 La Garde Cedex, France.

<sup>2</sup> SA, CNRS, Institut Pierre Simon Laplace, Ecole Polytechnique, 91128 Palaiseau Cedex, France.  
E-mail: [guenard@lseet.univ-tln.fr](mailto:guenard@lseet.univ-tln.fr)

**Abstract:** This study investigates the fundamental processes involved in the severe Mistral's windstorm occurring during the MAP IOP 15 (from 06 to 09 November 1999). It is based on numerical high-resolution simulations performed with the RAMS non-hydrostatic model at 3 km resolution. The simulation is found able to capture the flow complexity both upstream of the Alps and in coastal regions affected by the Mistral. The simulations accurately reproduce dynamical and thermodynamical fields observed by the observational network consisting of two UHF wind profilers set up near Marseille and Toulon and two radiosoundings at Lyon and Nîmes. The model indicates that the Mistral is mainly governed by flow splitting and downslope accelerations occurring at different scales. Wave breaking are triggered above local topography resulting in hydraulic jumps that in turn induce two mountain wakes trailing from the Alps and the Massif Central. The flow is accelerated by channelling effects between these two wakes. The simulations therefore evidence that channelling effects by the Rhône valley do not explain the Mistral's dynamics, which are fundamentally three-dimensional, multi-scaled and formed by a multitude of orographic processes.

**Keywords** - Flow splitting, Low-level jet, Mountain wakes, RAMS

## 1. INTRODUCTION

A severe Mistral event has been documented by two UHF wind profilers during the Mesoscale Alpine Program IOP 15 from the 6 to the 8 November 1999 (Guénard et al. 2005). The two wind profilers have been set up at the Rhône valley exit (STC), near Marseille, and downstream of the Alps (TLN) at Toulon (Fig. 1). This study aims at interpreting the time evolution of the wind profiles measured from the ground to 3 km AGL (above sea level) by means of high-resolution numerical simulations (3 km horizontal resolution) provided by the RAMS non-hydrostatic model.

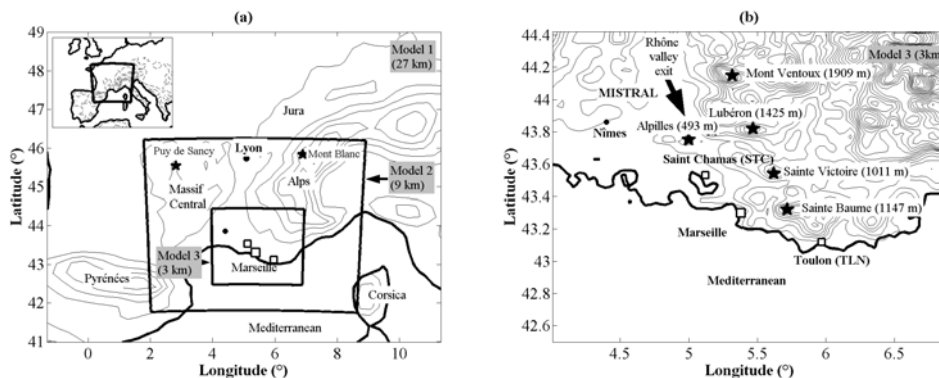


**Figure 1.** Target area in southeastern France and model grid divisions (from 27 to 3 km). Lyon and Nîmes are the radiosoundings locations. STC and TLN are the UHF wind profiler locations.

## 2. THE MISTRAL OBSERVATIONS

The synoptic environment is typical of a Mistral event. The Genoa cyclogenesis (1004 hPa) is initiated after the passage of a cold front from the Atlantic toward the Alps on 06 Nov. at 12 UTC. The Azores ridge (1028 hPa) over Spain strengthens the surface pressure gradient and the cyclone moves southeastward resulting in a strong northwesterly flow.

The two wind profilers show that a deep Mistral is triggered at the same time on 06 Nov. at 12 UTC (Fig. 2). Radiosondes at Nîmes (not shown), located farther on west from STC (Fig. 1b), indicate that the Mistral is 6 km deep. It evolves into a low-level jet on the 06 Nov. at 21 UTC at TLN (Fig. 2b) and on the 07 Nov. at 04 UTC at STC (Fig. 3a). The Mistral ends on 07 Nov. at 12 UTC at TLN and on 09 Nov. at 00 UTC at STC. The maximum wind speeds have reached  $40 \text{ m s}^{-1}$  at STC and  $30 \text{ m s}^{-1}$  at TLN.

Time-height diagrams of vertical velocity are presented for STC (Fig. 2c) and TLN (Fig. 2d). It can be first noted that  $w$  is contaminated by a rainfall occurring above the two sites on 06 Nov. at 09 UTC, visible by the large patch of intense negative  $w$ . The end of the rainfall coincides with the Mistral's onset. The  $w$  vertical profiles reveal that the air masses are globally subsident during the Mistral's activity.  $w$  is stronger above TLN (from  $-1$  to  $-2 \text{ m s}^{-1}$ ) than above STC (from  $-0.5$  to  $-1 \text{ m s}^{-1}$ ). A patch of relatively strong positive  $w$  values (around  $+1 \text{ m s}^{-1}$ ) is nevertheless observed on 07 Nov. at 03 UTC above 0.75 km AGL at STC (Fig. 2c). After the Mistral's breakdown at TLN on 07 Nov. at 12 UTC, positive  $w$  values (around  $+0.5 \text{ m s}^{-1}$ ) are also observed.

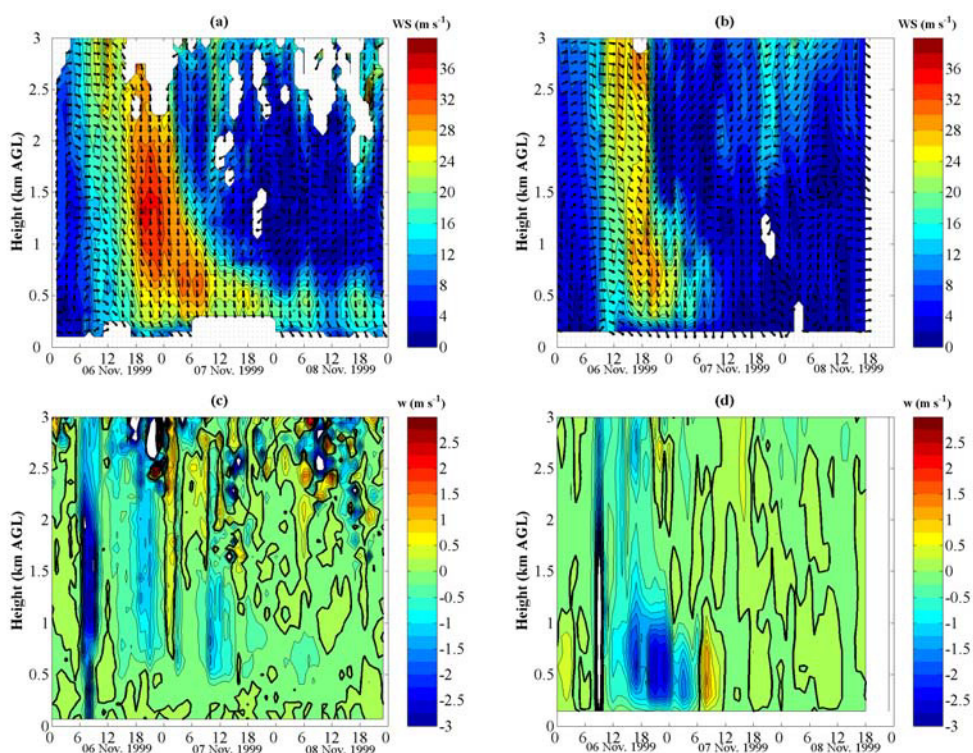


**Figure 2.** Time-height diagrams observed from 06 to 09 Nov. at 00 UTC. WS ( $\text{m s}^{-1}$ ) and WD ( $^{\circ}$ ) at (a) STC and (b) TLN.  $w$  ( $\text{m s}^{-1}$ ) at (c) STC and (d) TLN: bold lines contour the surface  $w = 0 \text{ m s}^{-1}$ .

## 3. THE RAMS SIMULATIONS

High-resolution numerical simulations have been performed with the non-hydrostatic RAMS model (Pielke et al. 1992). The simulations use three nested grids with 27, 9 and 3 km horizontal resolutions (see Fig. 1 for the model coverage). RAMS is nested into the ECMWF analyses giving its initial and boundary conditions every 6 hours. The simulation has been initialized on 05 Nov. at 00 UTC and has been integrated over 96 h.

The numerical results have been validated through direct comparisons against the UHF and radiosonde (RS) available observations. The comparisons involve the horizontal wind speed WS and direction WD (RS+UHF), the vertical velocity  $w$  (UHF), the relative humidity RH and the virtual potential temperature  $\theta_v$  (RS) vertical profiles. The validation is not detailed here.

The model simulations are in good agreement with observations in retrieving the transition from a deep to a shallow Mistral. The simulation correctly reproduces the intensity of the wind (maximum wind speed at STC  $\sim 35 \text{ m s}^{-1}$ ,  $\sim 30 \text{ m s}^{-1}$  at TLN) as well as the vertical velocity fields (maximum vertical velocity are underestimated by  $0.5 \text{ m s}^{-1}$  at TLN). RH and  $\theta_v$  have been also well reproduced with a bias of 15 % and 2 K respectively. The early Mistral's breakdown at TLN after a shallow phase is accurately simulated by the model. The persistence of the Mistral's low-level jet at STC is successfully captured by RAMS. At this step, it can be assumed that the RAMS simulations capture the dynamics of this Mistral event. The early cessation of the Mistral at TLN and the wind persistence of the STC low-level jet are now examined with the numerical simulations.

#### 4. WAKE BREAKING DOWNSTREAM OF THE ALPS

The vertical cross-section of the WS and  $\theta_v$  upstream of TLN on 07 Nov. at 00 UTC (Fig. 3c), clearly shows descending isentropes over the lee slopes of the Sainte Baume. A hydraulic jump occurs near the wind profiler associated with  $\text{TKE} \sim 3 \text{ m}^2 \text{ s}^{-2}$  (Fig. 3d) suggesting a gravity-wave breaking occurrence. The  $w$  cross-section (Fig. 3d) evidences the existence of mountain wave by the alternation of patches of upward and downward motions.  $w$  reaches  $-1.5 \text{ m s}^{-1}$  in agreement with the observations (Fig. 2d). Upward motions are simulated by the model after the wave breaking that likely explains the positive  $w$  values observed at TLN after the Mistral's breakdown (Fig. 2d). The breaking wave induces a mountain wake generating potential vorticity clearly visible on the surface wind fields at 0.5 km ASL (above sea level) on Fig. 3a and 3b. In fact, TLN is located at the exact position of the PV source. Farther downstream of TLN, positive and negative PV banners trail from the Sainte Baume with  $+4 \text{ pvu}$  and  $-2 \text{ pvu}$  respectively.

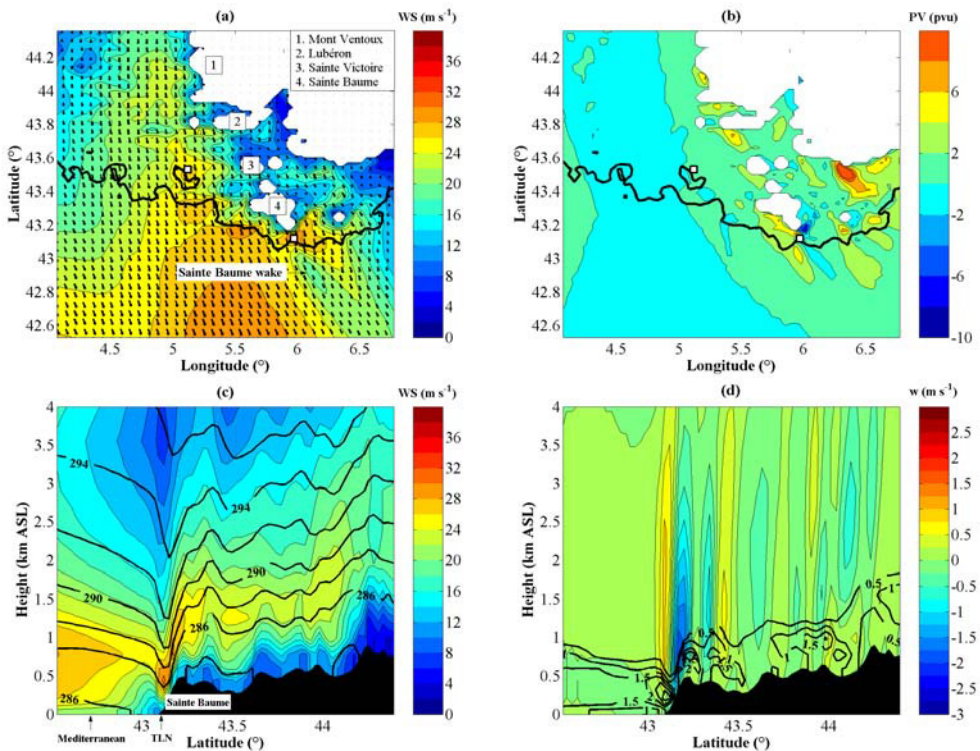


**Figure 3.** Simulated flow on 07 Nov. at 00 UTC. (a) Horizontal wind, in  $\text{m s}^{-1}$ , and (b) PV, in pvu, surface fields at 500 m AGL. South-North vertical sections crossing the TLN location in terms of (c) WS (colour scale) in  $\text{m s}^{-1}$  and  $\theta_v$  (solid lines) in K and (d)  $w$  (colour scale) in  $\text{m s}^{-1}$  and TKE (solid lines) in  $\text{m}^2 \text{ s}^{-2}$ .



## 5. FLOW SEPARATION AT THE EXIT OF THE RHONE VALLEY

The cross-section of the WS and  $\theta_v$  upstream of STC on 08 Nov. at 00 UTC (Fig. 4c) shows descending isentropes over the lee slopes of the Alpilles without hydraulic jump triggering.  $w$  values confirm lower vertical motions at STC ( $\sim -0.5 \text{ m s}^{-1}$ ) as observed by the wind profiler (Fig. 2c). The PV surface field at 0.5 km ASL (Fig. 4b) reveals that PV banners trail from the Massif du Lubéron and the Mont Ventoux. These PV filaments are generated by the flow separation mechanism. Their intensities are related to the primary PV banner induced by the Alps and to the incident flow as suggested by Aebischer and Schär (1998). Throughout the Mistral event, northwesterly to northeasterly incident flows prevail with a descending thermal inversion (from 3 km AGL on 07 Nov. at 00 UTC to 1 km AGL on 08 Nov. at 12 UTC, see Guénard et al. 2005). Thus, flow splitting occurs around the Alps during the deep Mistral phase leading to a large horizontal extension of the Mistral. As the incident thermal inversion height decreases, the flow splits around the less elevated peaks bordering the Rhône valley. It induces a flow confinement between the Alps wake and the Massif Central wake detailed by Jiang et al. (2003). The MAP IOP 15 Alps wake is not steady contrary to the wake documented during the MAP IOP 4 (Schär et al. 2003). The wake is induced by flow splitting around the Alps but also by wave breaking over local topography (for instance over the Sainte Baume).

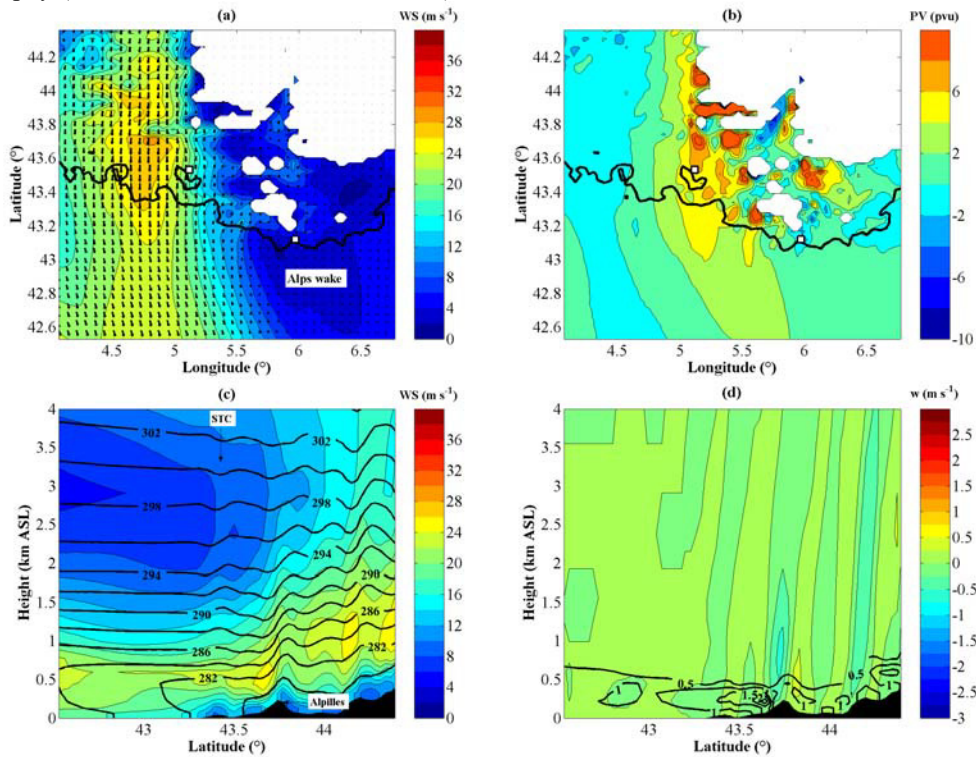


**Figure 4.** Simulated flow on 08 Nov. at 00 UTC. (a) Horizontal wind, in  $\text{m s}^{-1}$ , and (b) PV, in pvu, surface fields at 500 m AGL. South-North vertical sections crossing the STC location in terms of (c) WS (colour scale) in  $\text{m s}^{-1}$  and  $\theta_v$  (solid lines) in K and (d)  $w$  (colour scale) in  $\text{m s}^{-1}$  and TKE (solid lines) in  $\text{m}^2 \text{s}^{-2}$ .

## 6. CONCLUSIONS

The study has shown that the low-level jets observed at Saint Chamas and Toulon result from different mechanisms. The transient low-level jet observed at Toulon is induced by wave breaking over the Sainte Baume in response to a downslope flow. The low-level jet observed at Saint Chamas is mainly due to flow splitting around the Massif du Lubéron and the Mont Ventoux. This process involves channelling low-level accelerations between two wakes trailing from the Massif Central and the Alps. Downslope flows are also triggered over the Alpilles without gravity-wave breaking. The study highlights the flow

complexity mainly attributed to multi-scale interactive processes that make difficult the forecasting of the fine-scale dynamics of the Mistral.

**Acknowledgement:** *This work is supported by the Université du Sud Toulon-Var. The authors have appreciated the logistical support of Météo-France, Degréane Horizon and EDF during the MAP experiment. The authors are also thankful for all the efforts made by the MAP, the RAMS and the ECMWF communities.*

## REFERENCES

Aebischer, U. and C. Schär, 1998: Low-level potential vorticity and cyclogenesis to the lee of the Alps. *J. Atmos. Sci.*, **55**, 186-207.

Guénard V., P. Drobinski, J. L. Caccia, B. Campistron, and B. Bénéch, 2005: An observational study of the Mistral mesoscale dynamics. *Bound.-Layer Meteor.*, **115**, 263-288.

Jiang, Q., R. B. Smith and J. D. Doyle, 2003: The nature of the Mistral: Observations and modelling of two MAP events. *Quart. J. Roy. Meteor. Soc.*, **129**, 857-876.

Pielke, R.A., and Coauthors 1992: A comprehensive meteorological modelling system - RAMS. *Meteor. Atmos. Phys.*, **49**, 69-91.

Schär, C., M. Sprenger, D. Luthi, Q. Jiang, R. B. Smith, and R. Benoit, 2003: Structure and dynamics of an Alpine potential vorticity banner. *Quart. J. Roy. Meteor. Soc.*, **129**, 857-876.